ACS APPLIED MATERIALS & INTERFACES
Letter
www.acsami.org

Cobalt Hexacyanoferrate Nanoparticles as a High-Rate and Ultra-Stable Supercapacitor Electrode Material

Feipeng Zhao, Yeyun Wang, Xiaona Xu, Yiling Liu, Rui Song, Guang Lu, and Yanguang Li*

Institute of Functional Nano & Soft Materials (FUNSOM) & Collaborative Innovation Center of Suzhou Nano Science and Technology, Soochow University, Suzhou 215123, China

Supporting Information

ABSTRACT: Although great recent efforts have been invested to improve the performance of supercapacitors, these energy storage devices still fall short of meeting our expectations because of their limited working voltage, insufficient cycle life, and high manufacturing cost. Here, we report the facile preparation of cobalt hexacyanoferrate (CoHCFe) nanoparticles, which have an analogous structure to Prussian blue but with many vacant ferricyanide sites. In 0.5 M Na_2SO_4, CoHCFe exhibits specific capacitance of >250 F/g, excellent rate capability, and ultrahigh cycling stability with capacitance retention of 93.5% after 5000 cycles. Furthermore, CoHCFe was paired up with a carbon black modified graphene (mRGO) negative electrode to form asymmetric supercapacitors. They deliver a wide working voltage of ~2.4 V in Na_2SO_4, large energy density and power density. Given its high electrochemical performance, chemical robustness, environmental benignity, ease of preparation and low cost, CoHCFe as well as other Prussian blue analogues clearly deserve more attention for future energy storage applications.

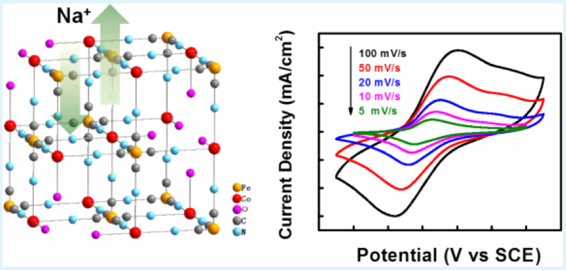

KEYWORDS: *cobalt hexacyanoferrate, Prussian blue, asymmetric supercapacitors, energy storage*

With the rapid development of the global economy, fossil fuels are on the verge of depletion. Tremendous efforts have been devoted to exploiting sustainable energy sources and advanced energy storage technologies.[1,2] Supercapacitors have attracted mounting attention as novel energy storage devices because of their high power densities and long cycle lives. These positive attributes make them promising in applications such as emergency power systems where high power delivery or uptake is needed.[3−5]

Typical electrode materials investigated for supercapacitors include carbonaceous or polymeric materials, metal oxides and hydroxides.[5] Encouraging progresses have been made over the past decade.[4−6] Nevertheless, some issues still persist. It remains a grand challenge to extend their limited working voltage, promote their insufficient energy/power density and cycle life, and lower their manufacturing cost.[5] In addition, many of these electrode materials are only operable in highly corrosive electrolytes, which are likely to cause corrosion damage to their closures. It is therefore more desirable to develop electrode materials operable in mild neutral electrolytes. Thus far, there have been few candidates available to meet this important criterion, two well-studied examples of which are carbon-based electrical double-layer capacitors and MnO_x-based faradaic pseudocapacitors.[7,8] The former suffer from the relatively low specific capacitance, whereas the latter are more or less restricted by their cycling stability.

Iron(III) hexacyanoferrate(II) or Prussian blue is one of the oldest known synthetic compounds. It has been widely applied as pigments or coating materials because of their high environmental compatibility and chemical stability.[9] Prussian blue and its analogues possess unique open framework structures with the general chemical formula of $A_hM_k[Fe(CN)_6]_l \cdot nH_2O$ (where A = alkali metal cation, M = transition metal cation).[9−11] The possibility to accommodate different transition metal cations within the coordination framework renders them with appealing electrochemical, ion-exchange, sensing, or photomagnetic properties, which have been the subject of intense research for decades.[9,11,12] Very recently, Prussian blue analogues have been investigated as the battery electrode materials.[13−16] They demonstrated decent specific capacity and excellent cycling stability. However, as far as we know, their potentials for supercapacitive energy storage have rarely been explored.[17] In this work, we prepared cobalt(II) hexacyanoferrate(III) (CoHCFe) nanoparticles as the supercapacitor electrode material in a neutral Na_2SO_4 electrolyte. This compound exhibited large faradaic capacitance under high current rates. When paired up with a graphene-based negative electrode in an asymmetrical supercapacitor, it delivered a high working voltage of ~2.4 V, remarkable energy/power density, and ultrahigh cycling stability.

For the synthesis of CoHCFe, an aqueous solution of $Co(NO_3)_2$ was added dropwise to an aqueous solution of $K_3Fe(CN)_6$ under vigorous magnetic stirring until a total molar ratio of Co:Fe = 3:2 was reached. During the course of

Received: May 30, 2014
Accepted: July 7, 2014
Published: July 7, 2014

ACS Publications © 2014 American Chemical Society

dx.doi.org/10.1021/am503375h | *ACS Appl. Mater. Interfaces* 2014, 6, 11007−11012

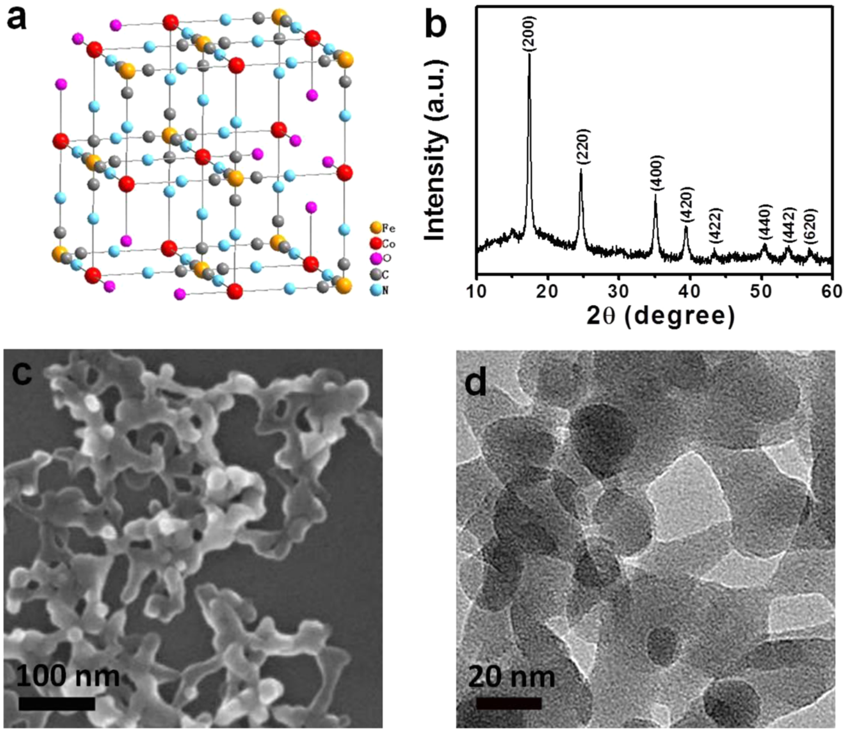

Figure 1. Crystal structure and morphology of CoHCFe nanoparticles. (a) Schematic of the CoHCFe crystal structure; (b) XRD pattern, (c) SEM image, and (d) TEM image of CoHCFe nanoparticles.

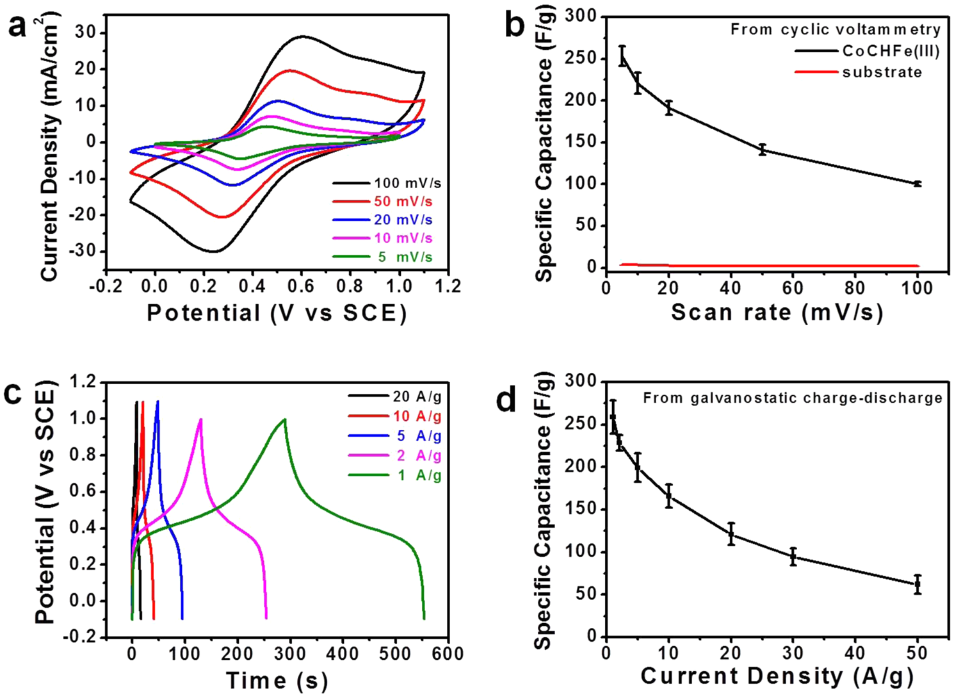

Figure 2. Supercapacitive performance of CoHCFe nanoparticles assessed from three-electrode measurements in 0.5 M Na_2SO_4. (a) CV curves at different scan rates; (b) specific capacitance derived from a; (c) galvanostatic charge–discharge curves at different current densities; (d) specific capacitance derived from c.

addition, reaction proceeded immediately as evidenced by the rapid formation of insoluble dark violet colloids. The resulting product was centrifuged, repetitively washed with copious amount of water, and finally lyophilized.

Figure 1b is the X-ray diffraction (XRD) pattern of CoHCFe. All the diffraction peaks are assignable to $Co_3(Fe(CN)_6)_2 \cdot xH_2O$ with no discernible impurity phase. Their broad width indicates the nanoscale feature of the final product. The stoichiometry agrees well with the starting molar ratio of the two metal precursors. Figure 1a schematically illustrates the possible crystal structure of CoHCFe. Analogous to Prussian blue, it has a three-dimensional cyano-bridged bimetallic basic unit with alternating Co(II) and Fe(III) located in a face-centered cubic lattice.[9−11] To maintain the specific stoichiometry, one-third of ferricynanide sites are unoccupied, resulting in a more open and accessible structure. There is no alkali metal cation in the tetrahedral sites of the cubic framework necessary for charge compensation.[11]

In images c and d in Figure 1, scanning electron microscope (SEM) and transmission electric microscope (TEM) were performed to interrogate the microstructure of CoHCFe. Nanoparticles of ∼20 nm in size are interconnected to form a continuous porous network. They appear to be poorly crystalline and gradually degrade under strong electron beam radiation. Prussian blue analogues are known to have rather limited thermal stability.[18] But at low temperatures (<100 °C) relevant to most battery or supercapacitor applications, its chemical stability is adequate.

The electrochemical performance of CoHCFe as a supercapacitor electrode material was first assessed by cyclic voltammetry (CV) and galvanostatic charge−discharge (CD) measurements in a three-electrode system in 0.5 M Na_2SO_4. Active material was blended with Super P conductive carbon black and polytetrafluoroethylene (PTFE) binder, and then loaded onto Ni foams to achieve a loading of 1 mg/cm^2 as the working electrode. Figure 2a shows the CV curves of the material at different scan rates within the potential window of −0.1−1.1 V versus saturated calomel electrode (SCE). A pair of pronounced redox peaks is located at ∼0.4 V. They correspond to the redox reaction of $Fe^{II/III}$ in CoHCFe, which is accompanied by Na^+ ion ingress in and out of the cyano-bridged metallic framework for maintaining local charge neutrality.[9,13] The symmetric peak shape indicates high reaction reversibility. Specific capacitance of CoHCFe was calculated and plotted with the scan rate in Figure 2b. At the slowest rate of 5 mV/s, it delivers a high value of 250 F/g, which is considerably larger than most carbon-based materials and closely approaching that of MnO_x.[7,8] The specific capacitance still retains >100 F/g under a high current rate of 100 mV/s. In order to exclude the possible contribution from the Ni foam substrate and conductive carbon additive, a control sample was prepared by loading Super P and PTFE alone on the working electrode, and measured under identical conditions. Negligible capacitance was recorded (Figure 2b). Furthermore, CoHCFe was also evaluated by charge/discharge experiments under different current densities from 1 A/g to 50 A/g (Figure 2c). These CD curves exhibit plateaus at 0.4−0.5 V, in accordance with the position of CV redox peaks. Their highly symmetric shapes reveal the high electrochemical reversibility and fast reaction kinetics. Specific capacitance estimated from CD curves is in the range of ∼250 F/g at 1 A/g to ∼60 F/g at 50 A/g (Figure 2d). At the maximum current rate of 50 A/g, the charge or discharge step is completed in less than 4 s. We also investigated higher loading of the active material up to 5 mg/cm^2 on the Ni foam substrate. The area-specific capacitance (in F/cm^2) increases almost linearly (see the Supporting Information, Figure S1).

For supercapacitors, good performance stability is another important criterion in the selection of electrode materials. The cycling stability of the CoHCFe was scrutinized from repetitive CV cycling. Its capacitance retention is derived and plotted with the cycle number (Figure 3). After 5000 potential cycles, more than 90% of the original capacitance was retained, underlining the ultrahigh chemical and structural robustness of the electrode material.

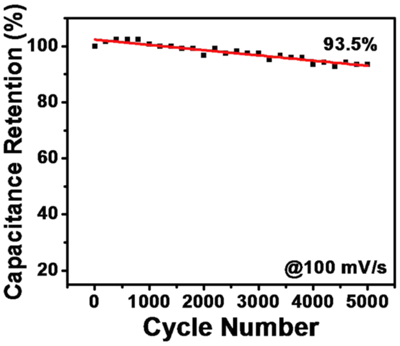

Figure 3. Potential cycling stability of CoHCFe nanoparticles.

The above electrochemical assessments reveal that our CoHCFe nanoparticles have large specific capacitance under high current rates and excellent cycling stability in Na_2SO_4. These properties, combined with the ease of preparation, make them a highly attractive candidate. Previously, attention has mostly been focused on carbon-based materials and MnO_x as supercapacitor electrode materials in neutral electrolytes. CoHCFe compares favorably to the former for its larger specific capacitance, and excel the later for its better chemical stability.[7,8,19−21] As for MnO_x, it is known to have a great propensity toward oxidation to form soluble Mn^{VII} (please refer to the Pourbaix diagram of manganese).

We explored the influence of Co(II) to Fe(III) molar ratio on the electrochemical performance of CoHCFe. The specific capacitance is found to rise considerably with Co amount from 1:1 to 3:2 (Figure 4a). Further increasing the ratio to 2:1 yields no obvious improvement. At the ratio of unity, CoHCFe is expected to adopt a perfect cubic framework free of vacant ferricyanide sites. Higher Co ratios bestow the crystal structure with increasing porosity and openness. This is evidenced by its much greater micropore Brunauer−Emmett−Teller (BET) surface area (see the Supporting Information, Figure S2). Previously, porous Prussian blue framework was observed to have higher storage capacity for hydrogen than their nonporous counterparts. A correlation was revealed between hydrogen uptake capacity and the concentration of framework vacancies.[22,23] Here, we believe that the structural nanoporosity also largely facilitate the transport of Na^+ ions in and out of CoHCFe framework. Moreover, Co(II)HCFe(II) nanoparticles were prepared from $K_4Fe(CN_4)_6$ and $Co(NO_3)_2$ at different Co to Fe ratios, but they were measured to have substantially lower specific capacitance (Figure 4b). Other bimetallic analogues MHCFe (M = Mn, Fe, Ni, Zn) were also attempted (see the Supporting Information, Figure S3). Among all the transition metals evaluated, CoHCFe exhibits the optimal activity. In addition, we examined the effect of other electrolyte cations (Li^+ or K^+) on the supercapacitive performance of CoHCFe. No obvious difference was noticed (see the Supporting Information, Figure S4).

In light of the great performance of CoHCFe in the positive potential regime, we decided to construct asymmetrical supercapacitors by pairing it with a negative electrode. Recently, graphene has received much attention for applications in energy storage by virtue of its large surface areas and high electric conductivity.[24,25] Unfortunately, exfoliated graphene sheets are highly likely to restack or aggregate, risking losing their nanoscale feature and surface areas.[26,27] To this end, we developed carbon black modified graphene sheets (mRGO, see

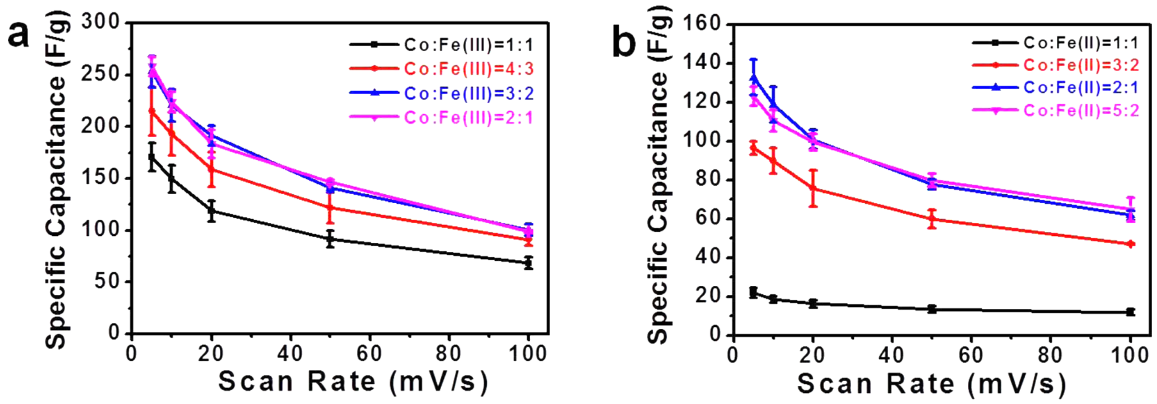

Figure 4. Influence of cobalt to iron molar ratio and iron oxidation state on the supercapacitive performance of CoHCFe. (a) Specific capacitance of Co(II)HCFe(III) nanoparticles with different starting Co(II) to Fe(III) molar ratios; (b) specific capacitance of Co(II)HCFe(II) nanoparticles with different starting Co(II) to Fe(II) molar ratios.

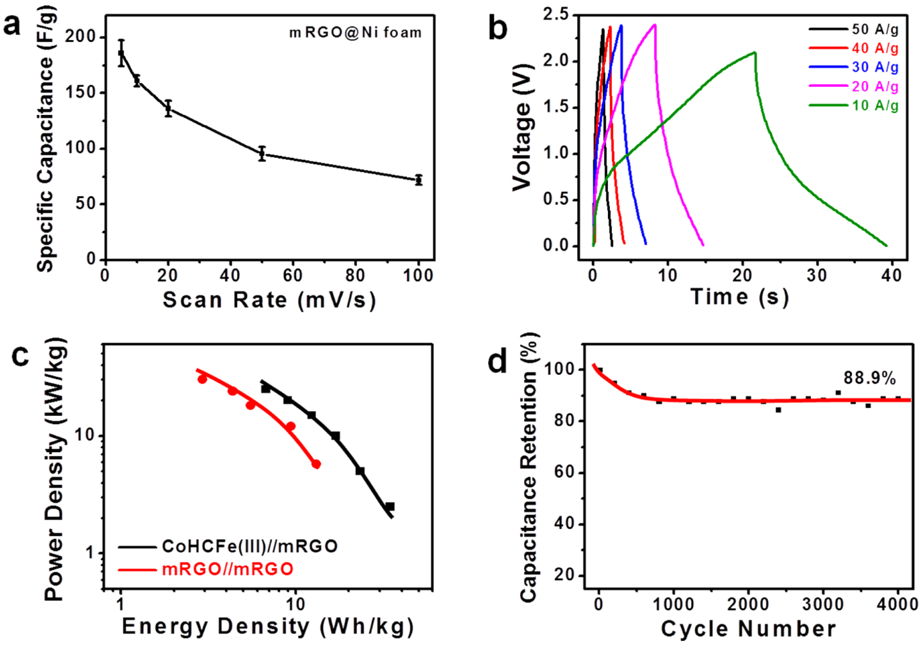

Figure 5. Performance of CoHCFe//mRGO asymmetric supercapacitors. (a) Specific capacitance of mRGO within the potential range of −1.1−0.1 V vs SCE at various scan rates. Data were derived from CV measurements; (b) galvanostatic charge−discharge curves of CoHCFe//mRGO asymmetrical supercapacitors at different current densities; (c) Ragone plot of CoHCFe//mRGO asymmetrical supercapacitors in comparison with mRGO/mRGO symmetrical supercapacitors; (d) cycling stability of CoHCFe//mRGO asymmetrical supercapacitor.

the Supporting Information for experimental details), in which carbon black nanoparticles were intentionally added as pillars between graphene sheets to effectively suppress their aggregation.[28] In such a configuration, the large surface areas of graphene sheets become more accessible. Indeed, mRGO exhibits improved specific capacitance than graphene alone, reaching ∼190 F/g at the scan rate of 5 mV/s and ∼70 F/g at 100 mV/s within a potential window of −1.1−0.1 V in 0.5 M Na_2SO_4 (Figure 5a).

For asymmetrical supercapacitors, CoHCFe positive electrode and mRGO negative electrode were paired up in a mass ratio of 1:1.4 to account for their difference in specific capacitance. They were galvanostatically charged and discharged in a two-electrode setup over a wide voltage range of 0−2.4 V (Figure 5b). It is worth noting that in most aqueous supercapacitors, the working voltage is limited to less than 2 V as restricted by the electrochemical stability window of water.[29] This is particularly severe for alkaline electrolytes as many faradaic supercapacitor electrode materials developed for those systems such as MnO_x and $Ni(OH)_2$ are also excellent electrocatalysts for water oxidation.[30,31] In the present work, our CoHCFe//mRGO asymmetrical supercapacitor can be charged up to ∼2.4 V as benefited from the ineffectiveness of CoHCFe and mRGO toward the electrocatalytic decomposition of water in Na_2SO_4. It presents a very important advantage in practical applications which demands higher working voltages. In Figure 5c, we depict the specific energy density and power density of the CoHCFe//mRGO asymmetric supercapacitor in the Ragone plot. It delivers a high energy density of 34.4 Wh/kg at a power density of 2.5 kW/kg, and a high power density of 25 kW/kg at an energy density of 6.7 Wh/kg. The maximum value of energy density is superior to that of most asymmetric supercapacitors operating in neutral electrolytes owing to its higher working voltage.[32−38] As a comparison, we also prepared and evaluated a symmetric mRGO//mRGO pair under the same condition. Although it has comparable power density to CoHCFe//mRGO, its energy density is only half or one-third of the latter, highlighting the merit of using CuHCFe as the positive electrode material. Furthermore, CoHCFe//mRGO asymmetric supercapacitor demonstrates remarkable cycling stability. The overall capacitance retention drops slightly in the first 1000 cycles, then levels off and stays constant at ~90% of the original value even after 4000 cycles (Figure 5d).

In summary, we prepared CoHCFe nanoparticles via a facile coprecipitation method. The product possesses a three-dimensional cyano-bridged bimetallic framework analogous to Prussian blue but with many vacant ferricyanide sites. The structural openness facilitates the passage of charge balancing ions (such as Na^+) in and out of the framework, and therefore expedites the electrochemical redox reaction of CoHCFe. When evaluated as the supercapacitor electrode material using a three-electrode system in a mild and noncorrosive Na_2SO_4 electrolyte, CoHCFe exhibits large specific capacitance under high current rates. More impressive is its excellent cycle life as a result of its chemical and structural stability. In light of its great potential, we further constructed asymmetric supercapacitors by pairing the CoHCFe positive electrode with an mRGO negative electrode. They deliver incredible working voltage as large as ~2.4 V, energy density up to 34.4 Wh/kg, and power density up to 25 kW/kg. Given the ease of preparation and low costs, CoHCFe and other Prussian blue analogues may hold great promise for future energy storage applications.

■ ASSOCIATED CONTENT

Ⓢ Supporting Information

Experimental details, additional characterization, and electrochemical data. This material is available free of charge via the Internet at http://pubs.acs.org/.

■ AUTHOR INFORMATION

Corresponding Author

*E-mail: yanguang@suda.edu.cn.

Notes

The authors declare no competing financial interest.

■ ACKNOWLEDGMENTS

Y.L. acknowledges startup support from Soochow University, the Priority Academic Program Development of Jiangsu Higher Education Institutions (PAPD), and the Program for Jiangsu Specially-Appointed Professors.

■ REFERENCES

(1) Dresselhaus, M. S.; Thomas, I. L. Alternative Energy Technologies. *Nature* **2001**, *414*, 332−337.

(2) Dunn, B.; Kamath, H.; Tarascon, J.-M. Electrical Energy Storage for the Grid: A Battery of Choices. *Science* **2011**, *334*, 928−935.

(3) Winter, M.; Brodd Ralph, J. What are Batteries, Fuel Cells, and Supercapacitors? *Chem. Rev.* **2004**, *104*, 4245−4269.

(4) Wang, G. P.; Zhang, L.; Zhang, J. J. A Review of Electrode Materials for Electrochemical Supercapacitors. *Chem. Soc. Rev.* **2012**, *41*, 797−828.

(5) Simon, P.; Gogotsi, Y. Materials for Electrochemical Capacitors. *Nat. Mater.* **2008**, *7*, 845−854.

(6) Arico, A. S.; Bruce, P.; Scrosati, B.; Tarascon, J.-M.; van Schalkwijk, W. Nanostructured Materials for Advanced Energy Conversion and Storage Devices. *Nat. Mater.* **2005**, *4*, 366−377.

(7) Zhang, L. L.; Zhao, X. S. Carbon-Based Materials as Supercapacitor Electrodes. *Chem. Soc. Rev.* **2009**, *38*, 2520−2531.

(8) Wei, W. F.; Cui, X. W.; Chen, W. X.; Ivey, D. G. Manganese Oxide-Based Materials as Electrochemical Supercapacitor Electrodes. *Chem. Soc. Rev.* **2011**, *40*, 1697−1721.

(9) Itaya, K.; Uchida, I.; Neff, V. D. Electrochemistry of Polynuclear Transition-Metal Cyanides - Prussian Blue and Its Analogs. *Acc. Chem. Res.* **1986**, *19*, 162−168.

(10) Buser, H. J.; Schwarzenbach, D.; Petter, W.; Ludi, A. Crystal-Structure of Prussian Blue - $Fe_4[Fe(Cn)_6]_3.xH_2O$. *Inorg. Chem.* **1977**, *16*, 2704−2710.

(11) de Tacconi, N. R.; Rajeshwar, K.; Lezna, R. O. Metal Hexacyanoferrates: Electrosynthesis, in Situ Characterization, and Applications. *Chem. Mater.* **2003**, *15*, 3046−3062.

(12) Karyakin, A. A. Prussian Blue and Its Analogues: Electrochemistry and Analytical Applications. *Electroanalysis* **2001**, *13*, 813−819.

(13) Wessells, C. D.; Huggins, R. A.; Cui, Y. Copper Hexacyanoferrate Battery Electrodes with Long Cycle Life and High Power. *Nat. Commun.* **2011**, *2*, 550.

(14) Wang, L.; Lu, Y.; Liu, J.; Xu, M.; Cheng, J.; Zhang, D.; Goodenough, J. B. A Superior Low-Cost Cathode for a Na-ion Battery. *Angew. Chem., Int. Ed.* **2013**, *52*, 1964−1967.

(15) Yue, Y.; Binder, A. J.; Guo, B.; Zhang, Z.; Qiao, Z.-A.; Tian, C.; Dai, S. Mesoporous Prussian Blue Analogues: Template-Free Synthesis and Sodium-Ion Battery Applications. *Angew. Chem., Int. Ed.* **2014**, *53*, 3134−3137.

(16) Pasta, M.; Wessells, C. D.; Liu, N.; Nelson, J.; McDowell, M. T.; Huggins, R. A.; Toney, M. F.; Cui, Y. Full Open-Framework Batteries for Stationary Energy Storage. *Nat. Commun.* **2014**, *5*, 3007.

(17) Chen, J.; Huang, K. L.; Liu, S. Q.; Hu, X. Electrochemical Supercapacitor Behavior of $Ni_3(Fe(CN)_6)_2(H_2O)$ Nanoparticles. *J. Power Sources* **2009**, *186*, 565−569.

(18) Allen, J. F.; Bonnette, A. K. Thermal-Decomposition of Prussian Blue - Isotopic Labeling with Mossbauer-Inactive Fe-56. *J. Inorg. Nucl. Chem.* **1974**, *36*, 1011−1016.

(19) Ko, W.-Y.; Chen, L.-J.; Chen, Y.-H.; Chen, W.-H.; Lu, K.-M.; Yang, J.-R.; Yen, Y.-C.; Lin, K.-J. One-Step Solvothermal-Processed 3D Spinel-Type Manganese Oxide Microspheres and Their Improved Supercapacitive Properties. *J. Phys. Chem. C* **2013**, *117*, 16290−16296.

(20) Qu, J.; Gao, F.; Zhou, Q.; Wang, Z.; Hu, H.; Li, B.; Wan, W.; Wang, X.; Qiu, J. Highly Atom-Economic Synthesis of Graphene/Mn_3O_4 Hybrid Composites for Electrochemical Supercapacitors. *Nanoscale* **2013**, *5*, 2999−3005.

(21) Wang, Y.; Chen, Q. Dual-Layer-Structured Nickel Hexacyanoferrate/MnO_2 Composite as a High-Energy Supercapacitive Material Based on the Complementarity and Interlayer Concentration Enhancement Effect. *ACS Appl. Mater. Interfaces* **2014**, *6*, 6196−6201.

(22) Kaye, S. S.; Long, J. R. The Role of Vacancies in the Hydrogen Storage Properties of Prussian Blue Analogues. *Catal. Today* **2007**, *120*, 311−316.

(23) Kaye, S. S.; Long, J. R. Hydrogen Storage in the Dehydrated Prussian Blue Analogues $M_3[Co(CN)_6]_2$ (M = Mn, Fe, Co, Ni, Cu, Zn). *J. Am. Chem. Soc.* **2005**, *127*, 6506−6507.

(24) Wang, H. L.; Dai, H. J. Strongly Coupled Inorganic-Nano-Carbon Hybrid Materials for Energy Storage. *Chem. Soc. Rev.* **2013**, *42*, 3088−3113.

(25) Sun, Y.; Wu, Q.; Shi, G. Graphene Based New Energy Materials. *Energy Environ. Sci.* **2011**, *4*, 1113−1132.

(26) Yang, X. W.; Zhu, J. W.; Qiu, L.; Li, D. Bioinspired Effective Prevention of Restacking in Multilayered Graphene Films: Towards the Next Generation of High-Performance Supercapacitors. *Adv. Mater.* **2011**, *23*, 2833−2838.

(27) Stankovich, S.; Dikin, D. A.; Piner, R. D.; Kohlhaas, K. A.; Kleinhammes, A.; Jia, Y.; Wu, Y.; Nguyen, S. T.; Ruoff, R. S. Synthesis of Graphene-Based Nanosheets via Chemical Reduction of Exfoliated Graphite Oxide. *Carbon* **2007**, *45*, 1558−1565.

(28) Yan, J.; Wei, T.; Shao, B.; Ma, F.; Fan, Z.; Zhang, M.; Zheng, C.; Shang, Y.; Qian, W.; Wei, F. Electrochemical Properties of Graphene Nanosheet/Carbon Black Composites as Electrodes for Supercapacitors. *Carbon* **2010**, *48*, 1731−1737.

(29) Wang, F. X.; Xiao, S. Y.; Hou, Y. Y.; Hu, C. L.; Liu, L. L.; Wu, Y. P. Electrode Materials for Aqueous Asymmetric Supercapacitors. *RSC Adv.* **2013**, *3*, 13059−13084.

(30) Gao, M.; Sheng, W.; Zhuang, Z.; Fang, Q.; Gu, S.; Jiang, J.; Yan, Y. Efficient Water Oxidation Using Nanostructured α-Nickel-Hydroxide as an Electrocatalyst. *J. Am. Chem. Soc.* **2014**, *136*, 7077−7084.

(31) Huynh, M.; Bediako, D. K.; Nocera, D. G. A Functionally Stable Manganese Oxide Oxygen Evolution Catalyst in Acid. *J. Am. Chem. Soc.* **2014**, *136*, 6002−6010.

(32) Lei, Z.; Zhang, J.; Zhao, X. S. Ultrathin MnO_2 Nanofibers Grown on Graphitic Carbon Spheres as High-Performance Asymmetric Supercapacitor Electrodes. *J. Mater. Chem.* **2012**, *22*, 153−160.

(33) Wu, S.; Chen, W.; Yan, L. Fabrication of a 3D MnO_2/Graphene Hydrogel for High-Performance Asymmetric Supercapacitors. *J. Mater. Chem. A* **2014**, *2*, 2765−2772.

(34) Wang, Q.; Yan, J.; Wang, Y.; Wei, T.; Zhang, M.; Jing, X.; Fan, Z. Three-Dimensional Flower-like and Hierarchical Porous Carbon Materials as High-Rate Performance Electrodes for Supercapacitors. *Carbon* **2014**, *67*, 119−127.

(35) Chen, L.-F.; Huang, Z.-H.; Liang, H.-W.; Guan, Q.-F.; Yu, S.-H. Supercapacitors: Bacterial-Cellulose-Derived Carbon Nanofiber@ MnO_2 and Nitrogen-Doped Carbon Nanofiber Electrode Materials: An Asymmetric Supercapacitor with High Energy and Power Density. *Adv. Mater.* **2013**, *25*, 4816.

(36) Gao, H.; Xiao, F.; Ching, C. B.; Duan, H. High-Performance Asymmetric Supercapacitor Based on Graphene Hydrogel and Nanostructured MnO_2. *ACS Appl. Mater. Interfaces* **2012**, *4*, 2801−2810.

(37) Yu, G.-H.; Hu, L.-B.; Vosgueritchian, M.; Wang, H.-L.; Xie, X.; McDonough, J. R.; Cui, X.; Cui, Y.; Bao, Z.-N. Solution-Processed Graphene/MnO_2 Nanostructured Textiles for High-Performance Electrochemical Capacitors. *Nano Lett.* **2011**, *11*, 2905−2911.

(38) Cheng, Y.; Zhang, H.; Lu, S.; Varanasi, C. V.; Liu, J. Flexible Asymmetric Supercapacitors with High Energy and High Power Density in Aqueous Electrolytes. *Nanoscale* **2013**, *5*, 1067−1073.